



Antibacterial, highly hydrophobic and semi transparent Ag/plasma polymer nanocomposite coating on cotton fabric obtained by plasma based co-deposition

Muhammad Irfan · Oleksandr Polonskyi · Alexander Hinz · Chiara Mollea · Francesca Bosco · Thomas Strunskus · Cristina Balagna · Sergio Perero · Franz Faupel · Monica Ferraris

Received: 19 March 2019 / Accepted: 13 August 2019 / Published online: 16 August 2019
© Springer Nature B.V. 2019

Abstract This study aims at deposition and characterization of antibacterial, hydrophobic and semitransparent metal/plasma polymer nanocomposite coating, containing Ag nanoparticles, onto cotton fabrics intended to be used in medical applications. The nanocomposite coatings were obtained via a simple, one step and ecofriendly plasma based co-deposition approach where silver was magnetron sputtered simultaneously with plasma polymerization of hexamethyldisiloxane (HMDSO) monomer. The nanocomposite thin films containing different concentration of silver were deposited either by varying silver sputter rate or thickness of the plasma polymer matrix to obtain a good balance between optical properties of the coated fabric and its long term antibacterial performance. The obtained coatings were

investigated in detail with respect to their composition, morphology, optical properties, nanoparticle size distribution, silver ion release efficiency, antibacterial performance, water contact angle and washing stability of the coating. The thickness of the plasma matrix was found to be more important in controlling the release of silver ions as well as affecting the optical properties of the coating. The water contact angle on the coated fabric was up to 145°, close to super hydrophobicity. The coating showed effective antibacterial efficacy against *Staphylococcus epidermidis* (a Gram positive bacterium) which was present even when fabric was subjected to 10 repeated washing cycles indicating good washing stability of the coating.

Keywords Plasma polymerization · Sputtering · Silver nanoparticles · Plasma polymer · Optical properties · Silver ion release properties

M. Irfan · C. Mollea · F. Bosco · C. Balagna · S. Perero · M. Ferraris
Department of Applied Science and Technology,
Politecnico di Torino, Corso Duca degli Abruzzi 24,
10129 Turin, Italy

O. Polonskyi · A. Hinz · T. Strunskus · F. Faupel
Chair for Multicomponent Materials, Faculty of
Engineering, Kiel University, Kaiserstr. 2, 24143 Kiel,
Germany

M. Irfan (✉)
Department of Materials and Testing, National Textile
University, Sheikhpura Road, Faisalabad 37610,
Pakistan
e-mail: see_irfan@hotmail.com

Introduction

Medical textiles used in the health care infrastructures are an important potential source of nosocomial infections. In general, bacterial infections pose a great threat worldwide not only to the public health but also to the economy as they elongate the average hospitalization period along with other associated costs. Since textiles are in close contact with human body, they

should not be a source of transmitting infectious diseases to patients or health care workers (Perelshtein et al. 2015). On the other hand, because of their greater surface area as well as ability to retain moisture, textiles provide a conducive environment for microorganisms to grow. Being closer to the skin of the wearer, they can contribute to the cross-contamination of pathogenic bacteria (Brunon et al. 2011) in different environments like home, hospitals and food industry where textiles are used immensely (Chadeau et al. 2010). Particularly, fabrics made of cellulosic fibers, for example cotton fabric, are more susceptible to microbial growth than synthetic fibers due to their ability to retain moisture. However, cotton fabrics provide superior comfort properties and thus are used widely not only in traditional textiles but also in medical textiles (Fei et al. 2018). This necessitates antibacterial functionalization of the textile surfaces and provides an impetus for research in antibacterial textiles. Consequently, research output regarding antibacterial functionalization of textile surfaces has increased tremendously.

Various antibacterial agents have been studied for imparting antibacterial functionality to textile surfaces which include organic antibacterial agents e.g. quaternary ammonium compounds (Lin et al. 2018), chitosan (Zemljič et al. 2017) and its derivatives (Stawski et al. 2016), N halamines (Liu et al. 2015), triclosan (Foksowicz-Flaczyk et al. 2016), polybiguanides (Gao and Cranston 2010), inorganic antibacterial agents e.g. Ag (Xu et al. 2017) and Pt and Zn (Ponomarev et al. 2018) nanoparticles, CuO (El-Nahhal et al. 2018), ZnO (Ghayempour and Montazer 2017) and natural antibacterial agents e.g. natural dyes (Mariselvam et al. 2017), curcumin (Pisitsak and Ruktanonchai 2014), aloe vera (Ali et al. 2014) and other plant extracts (Savoia 2012). Among these, silver nano particles are attractive because of their antimicrobial performance against a wide variety of bacteria and fungi (Wu et al. 2018). Although cytotoxicity of metal nanoparticles is a matter of concern, however, silver nanoparticles are considered less toxic to humans at lower concentrations (Jamuna-Thevi et al. 2011). Most of the wet chemistry routes for the synthesis and application of silver nano particles to textiles have disadvantages of agglomeration, non-uniform dispersion, use of expensive (and sometimes toxic) chemicals and complex chemical processes (Wu et al. 2018) as well as have

environmental concerns. Additionally, wet treatments may require higher quantities of antibacterial agents for achieving maximum antibacterial activity resulting in high weight add-on on the fabric. Lin et al. (2018) reported 8% weight add-on on pristine cotton fabric after coating polymeric antibacterial agent to achieve 100% bacterial reduction. The treatment was also reported to cause 6% reduction in the air permeability of the cotton fabric due to blockage of interfiber spaces.

Alternatively, plasma based processes including plasma polymerization and sputtering are increasingly being studied for textile surface functionalization due to their environment friendly nature as well as their ability to modify only the surface of the textiles while preserving their bulk properties (Irfan et al. 2017). Various plasma techniques (sputtering, plasma polymerization etc.) can be used separately or in combination to fabricate metal nanoparticles embedded in a matrix (Kratochvíl et al. 2018). Among these, nano composite films composed of silver nano particles embedded in a matrix, obtained by co-sputtering or sputtering and plasma polymerization, have been studied extensively because of their interesting functional properties (Hlídek et al. 2009). Nano composite films comprising metal nano particles embedded in an inorganic matrix are relatively simpler to obtain via co-sputtering (Irfan et al. 2017) than those where metal particles are embedded in a plasma polymerized matrix. Hexamethyldisiloxane (HMDSO) is the most commonly used plasma polymer precursor to fabricate nano composite coatings containing silver particles.

A variety of configurations of plasma techniques to obtain silver nanoparticles embedded in a plasma polymer matrix have been reported. These include single electrode deposition of both metal nanoparticles and polymer matrix (Hlídek et al. 2009; Despax and Raynaud 2007; Körner et al. 2010; Peter et al. 2011), fabrication of metal nanoparticles separately via gas phase condensation (GPC) (Schmittgens et al. 2009) or gas phase aggregation (Kuzminova et al. 2016; Kylián et al. 2017) of silver nano particles and various others configurations (Brunon et al. 2011; Beyene et al. 2010; Deng et al. 2014). Each technique has its own merits and demerits. In single electrode deposition, the deposition rate of silver and plasma polymer needs to be balanced to obtain homogeneous film due to silver target poisoning with plasma polymer (Körner et al. 2010; Peter et al. 2011). While the

synthesis of matrix and nanoparticles in separate plasma regions necessitates the instalment of additional gas phase aggregation or condensation source on the sputtering chamber (Schmittgens et al. 2009; Kuzminova et al. 2016).

Given the importance of aesthetic properties of textiles, transparent or semitransparent antibacterial coatings with effective broad spectrum antibacterial activity along with high washing stability has always been an area of interest for researchers. Nonetheless, for most of the coatings, a trade off is achieved between being antibacterial, transparent as well as having high washing stability. Silver nano materials are well-known antimicrobial agents effective against various types of microorganisms. However, whether incorporated within a polymer matrix (Ramirez and Jaramillo 2018) or coated on the surface of a substrate (Brunon et al. 2011), they impart color to the matrix or substrate due to surface plasmon resonance of the silver nanoparticles or clusters. There are studies reporting antibacterial textiles coated with silver nano particles/clusters with an acceptable level of transparency. Most of these approaches include lowering the silver concentration in the coating (Brunon et al. 2011; Chadeau et al. 2010) to reduce the intensity of surface plasmon resonance of the silver particles. But this can limit antibacterial performance or compromise long term antimicrobial activity which is associated with sustained release of silver ions (Körner et al. 2010) from the coating.

In this study nano composite coating consisting of silver nano particles embedded in plasma polymer matrix was deposited via a simple plasma based co-deposition scheme on a green colored cotton fabric meant to be used in medical applications. Separate power supplies to the two sputtering electrodes, along with other operational parameters, ensured independent control and manipulation of the matrix, silver nanoparticles amount, size and their distribution within the matrix with no observation of silver target poisoning. In addition, high deposition rates are possible to achieve. The matrix precursor monomer (HMDSO) was introduced, polymerized and deposited from the surface of an RF electrode whereas silver was simultaneously co-sputtered from DC electrode. Using this scheme, five different compositions of the composite coating were obtained by varying the silver concentration to have a balance between aesthetic look and antibacterial performance of the fabric. The silver

concentration was varied by two approaches to reduce the coloration of the fabric. In first approach, silver concentration was lowered to minimum in a 150 nm thick composite thin film. While in the second approach, silver dispersion was increased in a relatively thicker matrix while keeping the silver concentration per unit fabric area higher to get the benefit of reduced coloration combined with silver concentration enough for sustained silver ion release ability of the coated fabric. The obtained coatings were then investigated in detail for their morphology, composition, silver nano particle size and distribution, optical properties, potential of silver ion release, antibacterial effect against a Gram + bacterium and washing stability of the coating on the fabric.

Experimental

Method

The schematics of the deposition system used in this study is shown in Fig. 1. The system was composed of a main cylindrical ultra-high vacuum (UHV) chamber equipped with turbo molecular pump and rotary pump to create high vacuum. Two balanced magnetrons (Thin Film Consulting, ION'X-2UHV, diameter of 2 inch), one connected to the RF generator (13.56 MHz) and the other one connected to the DC power supply,

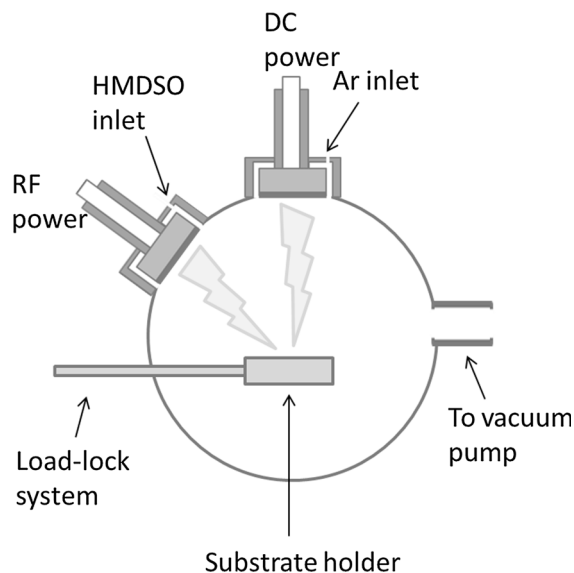


Fig. 1 Schematic of the deposition system

were installed on the main chamber. RF magnetron was used to deposit the plasma polymer and was equipped with a carbon target in order to prevent metal sputtering from the magnetron surface. DC magnetron was equipped with a silver target (2" dia, 99.99% Testbourne Ltd.) for sputter deposition of silver. The simultaneous deposition of silver and plasma polymer resulted in a nanocomposite thin film composed of plasma polymer matrix and silver nanoparticle inclusions. Due to independent power supplies, both the matrix thickness and silver concentration can be controlled separately. The matrix of the composite coating was obtained via plasma polymerization of the precursor hexamethyldisiloxane (HMDSO) which was introduced into the vacuum chamber through an inlet in the magnetron. Ar was used as working gas and was introduced in the chamber through an inlet in the DC magnetron. During simultaneous deposition, silver was deposited within the growing plasma polymer matrix on the surface of the substrate where nanoparticles are formed via self-organization. With the adopted scheme, no evidence of silver target poisoning due to plasma polymer sputtering was observed as has been reported in literature for such co-depositions (Drábik et al. 2015).

The silver concentration within the composite coating was varied by two different approaches: (1) by varying the deposition power of silver while keeping the coating thickness (or more accurately the matrix thickness) same or (2) by increasing the matrix thickness and keeping the silver deposition power constant. The objective of the two approaches was to obtain a balance between an acceptable level of transparency by reducing the silver concentration or particle size while maintaining long-term antibacterial effect. The second approach was adopted to get higher silver concentration on a unit fabric area with its expected properties of controlled release of silver ions from relatively thicker coating matrix that can prove beneficial for extended life of the coated fabric in repeated use or when subjected to multiple washing cycles.

In order to obtain the coatings with above two approaches, a composite coating with 150 nm thickness with maximum silver concentration obtained at silver sputtering power of 50 W was selected as starting point for this study. This starting point was selected after initial investigations keeping in view that even this maximum silver concentration did not

completely overshadow the green color of the cotton fabric in visual inspection thus preserving the original aesthetic look of the fabric to reasonable extent. The coating was obtained by applying a DC power of 50 W to silver and RF power of 25 W for HMDSO at 0.2 sccm monomer flow and 10 sccm Argon flow. Next, silver concentration in the coating was reduced either (1) by reducing silver sputtering power to 30 W and 15 W and keeping HMDSO deposition parameters the same or (2) by keeping the silver sputtering power at 50 W and increasing HMDSO flow (up to 0.5 sccm) to obtain greater dispersion of silver in a thicker matrix. The system was evacuated to a base pressure of about 3.0×10^{-4} Pa and deposition pressure was about 0.4 Pa. Table 1 summarizes the obtained coatings along with respective process which were deposited after preliminary investigations to find stable RF plasma discharge. The deposition time was kept constant for each deposition (10 min) with constant Ar flow (10 sccm). The samples are labelled by following the scheme (CF-coating thickness-silver sputtering power) where CF represents cotton fabric.

Characterization

Chemical composition of the deposited polymer matrix was analyzed using Fourier transform infrared reflection absorption spectroscopy (FTIR-RAS, Bruker Equinox 55). FTIR spectra were obtained for plasma polymer coatings deposited at 10, 25 and 50 W RF. Results were analyzed (discussed in the result section) and 25 W was selected to deposit plasma polymer throughout the study. In addition, FTIR spectra were also obtained for thicker polymer matrix obtained by increasing HMDSO flow while keeping RF power constant at 25 W. The spectra were obtained in the wave length range $500\text{--}4000\text{ cm}^{-1}$ and resolution of 4 cm^{-1} . For FTIR analysis, polymer coatings were deposited on gold coated silicon wafers.

Analysis of the surface chemistry of the cotton fabrics coated with nanocomposite films was performed using X-ray photoelectron spectroscopy (XPS, Omicron Nanotechnology GmbH) operating with Al anode at a power of 240 W. In order to detect the elements present on the surface the survey spectra were recorded (with pass energies of 100 eV). High-resolution spectra were obtained for the elements detected during survey scans using pass energy of 30 eV. The morphology of the composite coating was

Table 1 List of samples together with corresponding deposition conditions

Sample	RF power (W)	DC power (W)	Ar flow (sccm)	HMDSO flow (sccm)	Coating thickness (nm)	Silver filling factor (%)
CF-150 nm-50 W	25	50	10	0.2	150 ± 7	13
CF-150 nm-30 W	25	30	10	0.2	150 ± 5	8
CF-150 nm-15 W	25	15	10	0.2	150 ± 8	5
CF-300 nm-50 W	25	50	10	0.4	300 ± 10	8
CF-400 nm-50 W	25	50	10	0.5	400 ± 12	6

analyzed using scanning electron microscope (SEM, Zeiss Ultra Plus). Silver nano particle's shape and size distribution were determined using transmission electron microscopy (TEM, JEM-2100, JEOL, 200 kV, LaB6). TEM samples were prepared by depositing 25–30 nm of composite coating on carbon coated copper grids. The obtained images were processed by an image processing software ImageJ (ImageJ) and size histograms for silver nanoparticles were obtained.

Optical properties of the composite coating were assessed using UV–Vis spectroscopy (Ellipsometer Woollam M2000 UI). Coatings were deposited on quartz glass to obtain UV–Vis transmittance spectra in the wavelength range 250–1000 nm. The total concentration of the silver deposited under three silver sputtering powers (15 W, 30 W and 50 W) was determined through Inductively Coupled Plasma Mass Spectroscopy (ICP–MS, Thermo Scientific iCAPTM Q ICP–MS). For this purpose, coated cotton samples ($1 \times 1 \text{ cm}^2$) were dissolved in a mixture of nitric acid (65%) and H_2O_2 (30%). The liquor was then filtered. The instrument (ICP-MS) was calibrated using solution containing 125, 250, 500 and 1000 ppb of silver. The potential of the composite coatings to release silver ions in aqueous media was determined through silver ion release test. In silver ion release test, fabric samples ($1 \times 1 \text{ cm}^2$) were immersed in 10 ml water (milliQ) in small plastic bottles at room temperature. 1 ml water sample was drawn from the bottles after 3, 24 and 72 h and quantity of ionic silver leached from the fabric was determined through ICP–MS (Thermo Scientific iCAPTM Q ICP–MS). Three samples for

each coating were tested and average concentration was reported.

Antibacterial performance of the cotton fabric coated by nanocomposite thin film was assessed via “Inhibition halo test” performed against *Staphylococcus epidermidis* LMG 10474, a Gram positive bacterium. For the test, a bacterial inoculum was prepared by means of a water suspension of the colonies grown over night on Nutrient agar plate at 37 °C, the suspension was diluted to obtain a value of optical density at 620 nm (O.D._{620}) between 0.8 and 1. The suspension was spread on the surface of Mueller–Hinton agar plate by means of an inoculating loop. Coated and uncoated cotton fabric samples ($1 \times 1 \text{ cm}^2$) were placed in contact with the inoculated agar plates and incubated at 37 °C for 24 h. At the end of the incubation period the microbial growth was observed to identify the presence of the inhibition halo around the fabric samples and/or the lack of the growth under them.

In order to analyze the washing stability of the coating, the “Inhibition halo test” was also performed on coated fabric samples subjected to 10 washing cycles. Coated fabric samples of size $2 \times 2 \text{ cm}^2$ were washed in 100 ml water in a beaker. Washing was performed in a thermostat bath at 60 °C for 30 min with oscillations set at 150 per minute. Soap solution was composed of AATCC standard detergent without optical brightener (WOB) at a concentration of 2 g/l. Energy Dispersive X ray spectroscopy (EDX) was also performed on washed samples to assess the presence of the coating on fabric surface by detecting the elements of coating.

Finally, the water wettability of the coated fabric surface was determined with water contact angle method. A water droplet of 5 μl was dropped on the surface of the coated and uncoated fabric samples and image was captured after 10 s to measure contact angle. Five measurements were taken for each coating and average value of contact angle was reported.

Results and discussion

Compositional and morphological characterization

Infrared spectroscopy was employed to investigate the structure of the plasma polymer at different applied RF power for a given flow rate of HMDSO and at different flow rates of HMDSO at fixed applied power. Figure 2 shows FTIR spectra to identify different kinds of bonding in plasma polymerized HMDSO films according to literature (Despax and Raynaud 2007). The absorption band with the highest intensity is present at 1081 cm^{-1} which represents Si–O–Si asymmetric stretching vibration and may also be overlapped with CH_2 wagging band in the range $1040\text{--}1060\text{ cm}^{-1}$. This strong wagging band due to CH_2 is usually accompanied with CH_2 scissor vibrations which are represented by a small peak at 1357 cm^{-1} associated with Si– CH_2 –Si. This small peak originating due to Si– CH_2 –Si suggests that Si–

CH_2 –Si bridge building can be one of the mechanisms of plasma polymerization in the adopted deposition scheme (Rau and Kulisch 1994). The peak at 1460 cm^{-1} and at 1406 cm^{-1} are representative of CH_3 asymmetrical and symmetrical bending respectively and also points to the polymeric structure of the thin film. The absorption band present at 1700 cm^{-1} indicates presence of oxygen in C=O whereas a small peak at 1620 cm^{-1} represents contribution from C=C (Hanus et al. 2009). The absorption band at 2145 cm^{-1} represents Si–H bond (Rau and Kulisch 1994). The peak at 1260 cm^{-1} is due to Si– CH_3 derived from Si– $(\text{CH}_3)_2$ groups (Radeva et al. 2014). The peaks at 2966 cm^{-1} and 2902 cm^{-1} are representative of asymmetric and symmetric stretching vibrations of CH_2 in the Si– CH_2 –Si fragments. The absorption peak at 850 cm^{-1} can be associated with Si– CH_3 stretching vibration originating from Si– $(\text{CH}_3)_3$ end groups whereas a small shoulder peak in its vicinity appearing at 807 cm^{-1} can be assigned to stretching vibrations of the Si– CH_3 bond derived from Si– $(\text{CH}_3)_2$ and Si– CH_3 groups (Radeva et al. 2014). When power is increased from 10 to 25 and 50 W for a fixed monomer (HMDSO) flow of 0.2 sccm and constant Ar flow of 10 sccm, the intensity of the peak at 850 cm^{-1} reduced suggesting the removal of CH_3 groups, during plasma polymerization (Radeva et al. 2014). Since RF plasma at 25 W was found to be more stable than at 50 W, therefore, 25 W was selected for deposition of plasma polymerized HMDSO films along with co-sputtering of silver for the rest of the experiments. These results indicate successful plasma polymerization and deposition of $\text{SiC}_x\text{O}_y\text{H}$ films on the substrates. Moreover, the structure of the plasma polymer can be varied by the applied RF power.

The structure of the plasma polymer films can be varied either by changing the power (as discussed above) or by changing the monomer (HMDSO) flow rate. This can be seen from FTIR spectra of plasma polymer films obtained at increased HMDSO flow rate (0.4 and 0.5 sccm) at 25 W. Films obtained at increased HMDSO flow again exhibit an increased intensity at 850 cm^{-1} suggesting higher number of CH_3 groups due to increased monomer flow rate.

Further chemical characterization of the composite thin film coatings comprising silver nanoparticles embedded in the plasma polymer matrix and deposited onto cotton fabric was performed using XPS. Survey spectrum (not shown here) of the uncoated fabric

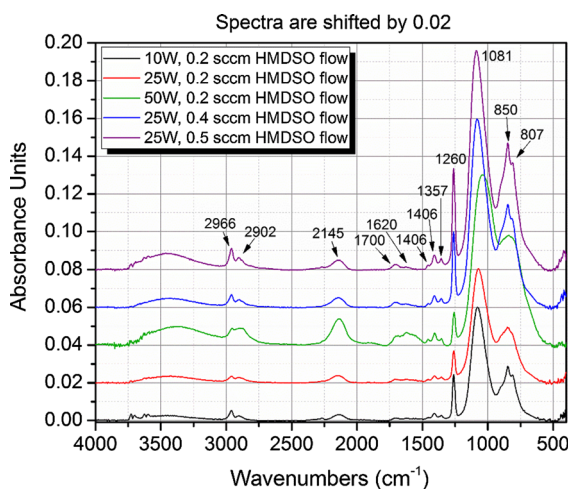


Fig. 2 FTIR spectra of plasma polymer thin films deposited onto gold-coated silicon wafers at different RF power and HMDSO flow rates. Ar flow was fixed at 10 sccm

surface indicated the presence of carbon and oxygen as these are the main constituents elements of cellulose fibers. Additionally, silver and silicon peaks appeared in the survey spectrum of the cotton fabric coated by nanocomposite thin film (Fig. 3a). For the detailed interpretation of XPS results only three samples with constant film thickness and different Ag content were selected. High resolution XPS spectra of O-1s, Si-2p and Ag-3d are shown in Fig. 3b–d, respectively. Their detailed analysis with respect to chemical shifts yields important information about the bonding between different elements present on the surface and, thus gives the information about the chemical structure of nanocomposite thin films. All XPS spectra

were charge referenced for aliphatic carbon at 285.0 eV. The O-1s peak located at around 532.8 eV represents O–Si bonds (Brunon et al. 2011) originating from organosilicon like structure (Alexander et al. 1996). Generally, high resolution O-1s XPS peaks for the three selected samples are almost identical, except only a small shift of the peak shoulder located at lower binding energy (~ 531.0 eV). More specific, this component of the peak is increasing with the increasing silver concentration in the nanocomposite films. Such peak can be attributed to Ag-oxide groups which are formed either due to formation of Ag–O bonds in the polymeric films or due to surface oxidation after the exposure to the atmosphere.

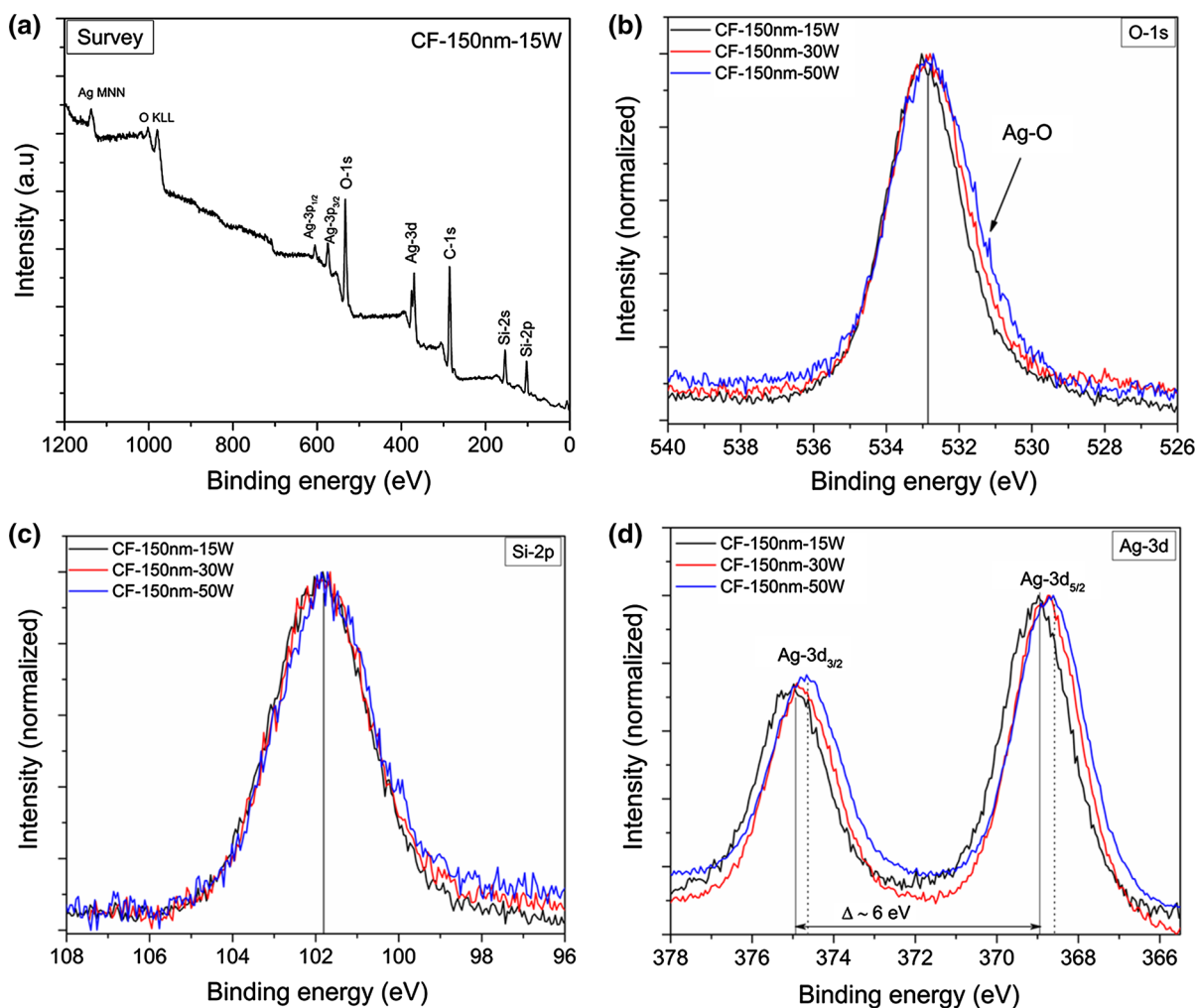


Fig. 3 XPS spectra for selected cotton fabric coated by nanocomposite thin films: **a** survey spectrum for CF-150 nm-15 W; **b–d** high resolution XPS spectra of O-1s, Si-2p and Ag-

3d peaks, respectively, for three selected samples with constant film thickness and various silver amount. All the high resolution spectra are normalized

High-resolution Si-2*p* peak, located at 101.8 eV can be assigned to Si atoms bonded to oxygen (correlation with O-1*s* interpretation, see above) as well as different hydrocarbons (FTIR spectra confirm similar observations). According to the literature, components of Si-2*p* peak located at 101.5, 102.1 and 102.8 eV have been reported to be originating from R₃SiO, R₂SiO₂ and RSiO₃ respectively (R being hydrocarbon) (Saulou et al. 2012). As one can notice from Fig. 3c all three Si-2*p* spectra for different samples are identical, suggesting that there is no influence of silver concentration on the chemical structure of the plasma polymerized HMDSO matrix.

Figure 3d shows a comparison of high resolution of Ag-3*d* for nanocomposite thin films containing different amount of Ag inclusions. For the sample with the lowest Ag concentration (CF-150 nm-15 W) Ag-3*d*_{5/2} peak positioned at 368.8 eV and Ag-3*d*_{3/2} peak at 374.8 eV with spin orbit separation of 6 eV suggest silver in metallic form (Ag⁰) (Deng et al. 2014). However, the comparison of Ag-3*d* peaks for samples with higher Ag amount shows a shift of the Ag peaks to lower binding energy by roughly 0.25–0.35 eV that might be an indication of a slight silver oxidation caused, most likely, by the exposure to the ambient atmosphere (Moulder and Chastain 1992).

Elemental atomic concentrations obtained from XPS measurements are also shown in the Table 2. The key information from the table is to confirm the presence and show variation of silver concentration on the surface of samples depending upon the deposition conditions. The surface silver concentration increases with increase in silver sputtering power for a given coating thickness and decreases with increase in coating thickness at a given silver sputtering power. The surface atomic percent of silver is 2.7, 4.9 and

8.7% when sputtered at 15 W, 30 W and 50 W respectively. When coating thickness was increased to 300 and 400 nm by increasing the HMDSO flow while maintaining the silver sputtering power at 50 W, the silver atomic percent on the surface decreases and comes closer to what was observed at 30 W (for 150 nm) and 15 W (for 150 nm). This is also in agreement of decreasing silver particle size (TEM micrographs) due to greater dispersion of the silver within the bulk of the thicker matrix.

Thus it can be concluded that plasma polymerization of HMDSO monomer resulted in an organosilicon like coating containing silver nanoparticles with surface silver concentration that increased or decreased depending upon the deposition conditions hence affecting the distribution of silver within the polymer matrix.

The morphology of the composite coatings deposited onto cotton fabric can be seen in SEM images shown in Fig. 4. The surface of the uncoated cotton fiber was relatively smooth showing original features of the fiber surface. After deposition of nanocomposite thin films, dense granular topography, typical for sputter deposited coatings (Irfan et al. 2017), can be seen on the surface of the fibers indicating presence of the coating. However, silver nanoparticles are not visible on the fiber surface. This is expected as silver nanoparticles are supposed to be embedded within the plasma polymer matrix according to the adopted deposition scheme. The SEM images show uniform and conformal coverage even on uneven fiber surfaces. Further, EDX analysis (not shown here) revealed the presence of the elements Ag, Si along with C and O. This confirms the presence of silver nanoparticles and organosilicon like polymer on coated cotton fibers.

Table 2 Elemental atomic percent from XPS for uncoated and coated cotton fabric

	Sample	C	O	Si	Ag
Fixed coating thickness and Increasing silver sputtering power	CF-uncoated	76.5	23.4	–	–
	CF-150 nm-15 W	53.3	24.0	20.0	2.7
	CF-150 nm-30 W	56.7	21.8	16.6	4.9
	CF-150 nm-50 W	55.8	20.6	14.9	8.7
Increasing coating thickness and fixed silver sputtering power	CF-150 nm-50 W	55.8	20.5	14.9	8.7
	CF-300 nm-50 W	50.4	23.9	21.1	4.6
	CF-400 nm-50 W	51.2	24.0	21.6	3.2

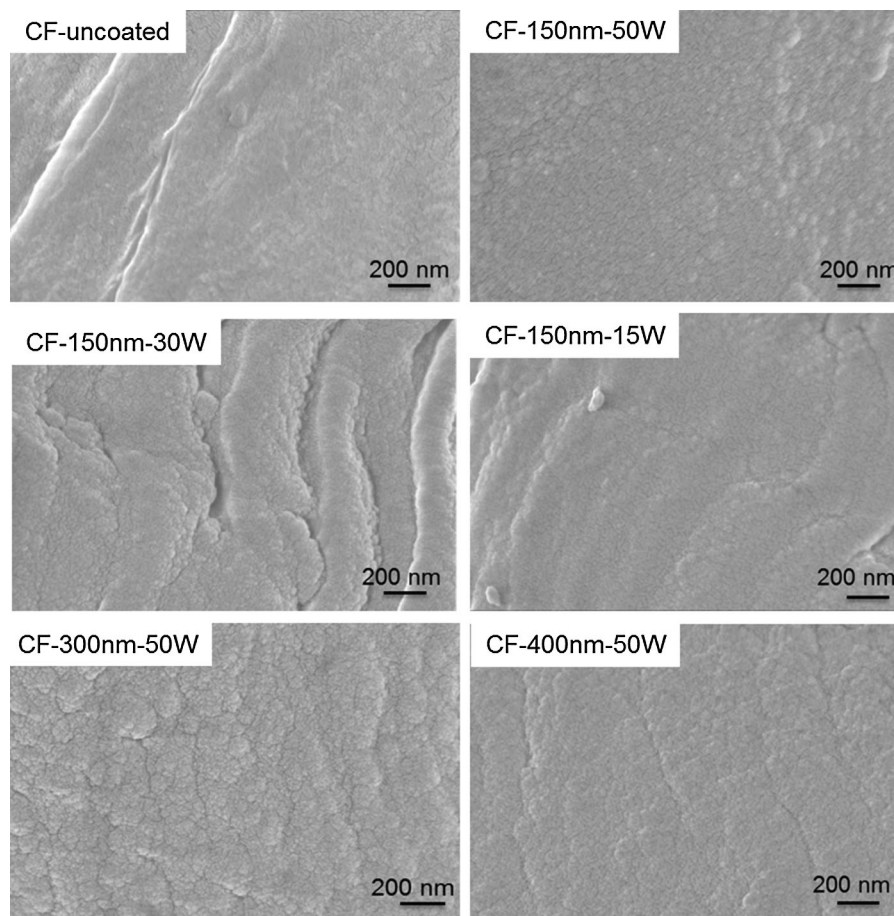
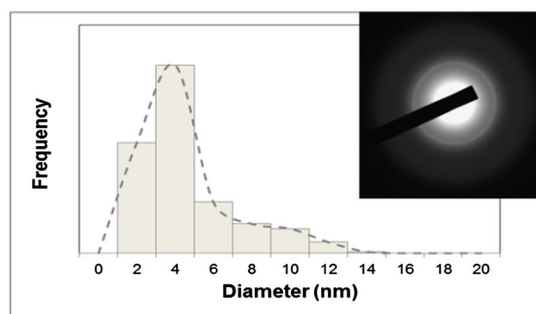
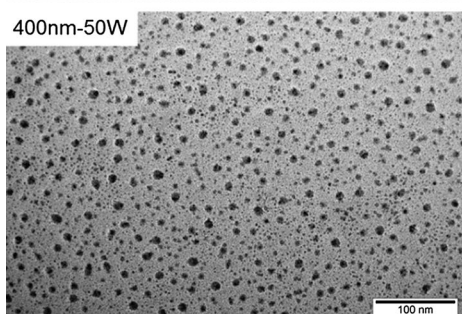
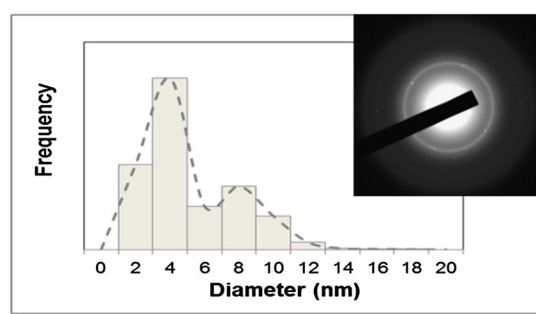
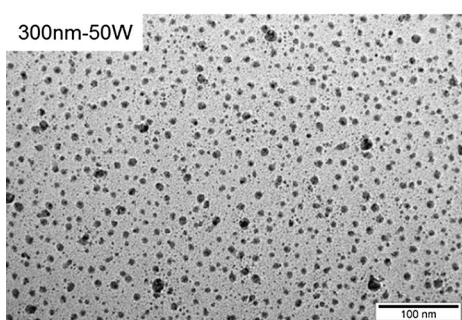
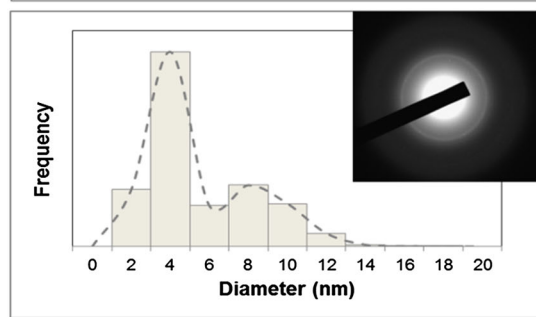
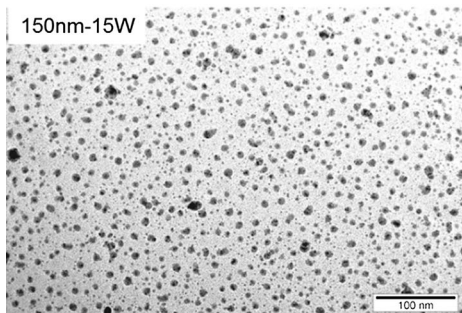
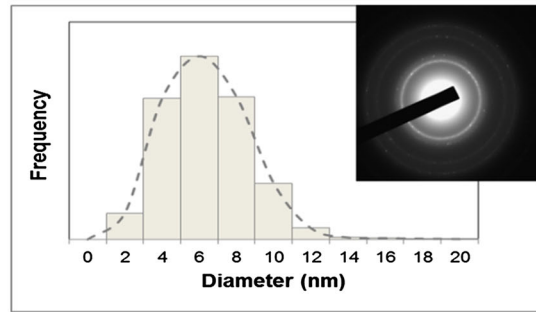
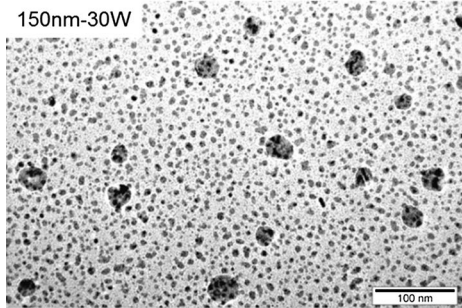
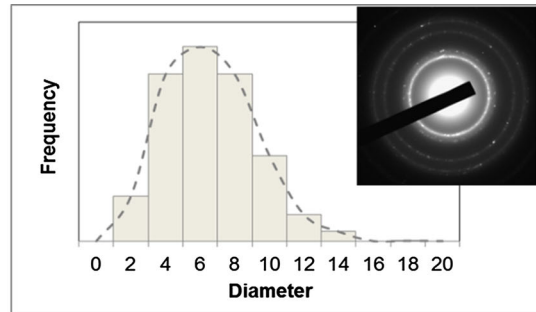
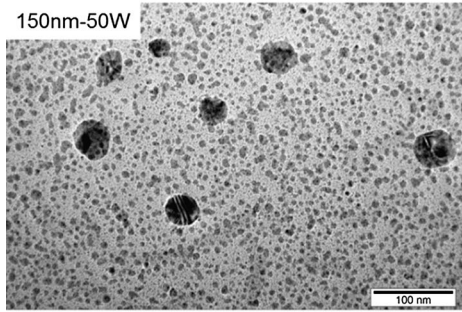


Fig. 4 High magnification SEM images of cotton fibers coated with nanocomposite thin films comprising silver nanoparticles embedded in plasma polymer matrix

TEM was performed to analyze the size of the silver nanoparticles and their distribution in the polymer matrix obtained under different deposition conditions and results are shown in Fig. 5. The size distribution of the silver nanoparticles was determined using image processing software ImageJ. The figure shows that spherical silver nanoparticles were homogeneously distributed within the amorphous plasma polymer matrix. However, some non spherical particles can also be seen at increased deposition power of silver (150 nm-50 W and 150 nm-30 W) which were formed due to coalescence of smaller particles within the growing polymer matrix as result of higher deposition rate of silver. In addition, under higher deposition powers of silver, few particles as large in diameter as 34 or 44 nm can also be observed in TEM micrograph shown in Fig. 5. At lower deposition power (150 nm-15 W), a bimodal size distribution

was observed with majority of the silver particles of 4 nm followed by 8 nm in size. With increase in silver sputtering power (150 nm-30 W and 150 nm-50 W) while keeping the deposition of the plasma polymer the same, an increase in the diameter of the nanoparticles can be observed from the size distribution histograms in Fig. 5. This results in normal distribution with maximum in size distribution at around ~ 6 nm with increase in silver sputtering power (150 nm-50 W).

When thickness of the plasma polymer matrix was increased by increasing the flow rate of the HMDSO monomer while keeping the silver sputtering power fixed at 50 W (300 nm-50 W), bimodal size distribution for silver nanoparticles was observed again. Since the nucleation of the metal nanoparticles and their growth is controlled by their surface diffusion coefficients in the plasma matrix (Drábik et al. 2015), the



◀ **Fig. 5** TEM images of composite coating deposited on TEM grids showing silver nanoparticles embedded within the plasma polymer matrix under different deposition conditions. Images were processed using ImageJ to produce size histograms

thicker plasma matrix may limit the diffusion of silver atoms reducing the size of the silver nanoparticles leading again to bimodal size distribution even at higher silver sputtering power. Thus, at thickness of 300 nm, the average diameter of the majority of the silver nanoparticles was around 4 nm followed by 8 nm in diameter. With further increase in matrix thickness to 400 nm (400 nm-50 W), a further increase in the number of silver particles of ~ 4 nm diameter occurred followed by an increase in number of even smaller nanoparticles of ~ 2 nm. An equivalent decrease in the number of nanoparticles with higher diameter of about 8 nm is also evident. Because of this reason, the average diameter of silver nanoparticles, reported in Fig. 5, decreased with decrease in silver sputtering power while it also decreased even to greater extent with increase in coating matrix thickness. In all the cases, the size of the majority silver nanoparticles varied between 2 and 14 nm which is similar to what has been reported earlier for the nano composite coating obtained under a different plasma configuration (Peter et al. 2011). The inset images in Fig. 5 show the selected area electron diffraction (SAED) pattern of the composite films. Well ordered diffraction rings visible as bright dots indicate the presence of crystalline silver nanoparticles (Drábik et al. 2015). These diffraction rings are more visible for the composite coating containing higher silver concentration and larger nanoparticles (150 nm-50 W, 150 nm-30 W) than those with lower silver concentration and smaller particles (150 nm-15 W, 300 nm-50 W, 400 nm-50 W). The variation in the size of the silver nanoparticles and their distribution was also reflected in the corresponding UV–Vis spectra of the composite coating obtained under different conditions as discussed below.

Optical properties

Optical properties of the composite coatings were evaluated with UV–Vis spectroscopy and results are shown in Fig. 6a, b. The transmittance spectra were acquired for different nanocomposite thin films

deposited onto quartz glass substrates. UV–Vis spectra are combined into two groups: (1) fixed total thickness of nanocomposite thin films with different Ag filling factor (Fig. 6a) and (2) constant Ag amount and varied thin film thickness (Fig. 6b). In both cases absorbance peaks with different intensities can be seen depending upon the total silver concentration as well as silver nanoparticle size distribution in accordance with TEM results. The spectrum of the quartz glass substrate coated with 150 nm thick plasma polymer only is shown for comparison purposes. The coating with minimum silver concentration resulted in maximum transmission. At lower deposition power (150 nm-15 W), silver nanoparticles have bimodal size distribution as discussed in the TEM analysis and hence exhibit two absorption peaks at around 345 and 420 nm. Traditionally, the optical absorption of metal nanoparticles is ascribed to be due to Localized Surface Plasmon Resonance (LSPR) (Wiley et al. 2006). However, due to intraband excitation of the conduction electrons by incident photons, it can also be described quantum mechanically. The maximum absorbance–wavelength, according to quantum theory of nanoparticles, is linked with the conduction band energy (Gharibshahi et al. 2017). Contrary to the bulk metals, conduction electrons are not completely free in metal nanoparticles rather some of them are linked with individual atoms while others are free to move. When photon of light hit the metal nanoparticles, these conduction electron get intra band excitations. Smaller sized particles are composed of fewer metal atoms which reduces the potential attraction between metal ions and conduction electrons in the nanoparticle. This leads to increased conduction band energy for smaller sized nanoparticles. On the other hand, larger particles are composed of greater number of metal atoms leading to increased attraction between conduction electrons and metal ions. Thus conduction band energy of larger sized particles is reduced (Gharibshahi et al. 2017). It has been reported that smaller sized silver particles (up to 2 nm) can exhibit more than one absorption peaks due to molecule-like optical transitions. As their size grows (> 2 nm), the absorption band is influenced by surface plasmon resonance of free electrons in the particles (Bakr et al. 2009).

With the increase in silver deposition power (150 nm-30 W and 150 nm-50 W), silver nanoparticle size and concentration increased, therefore, the absorption intensity increased significantly and shifted

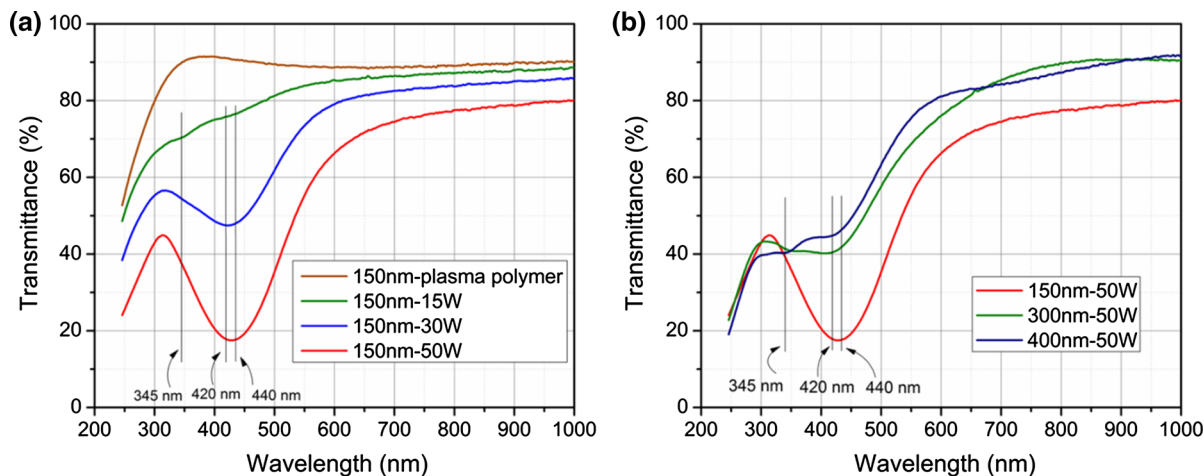


Fig. 6 Transmittance UV-Vis spectra of the Ag/ppHMDSO nanocomposite coatings deposited onto quartz glass: **a** constant thickness of nanocomposite thin film with different silver

from 420 to 440 nm whereas the absorption peak at 345 nm vanished giving rise to a broad single peak (Fig. 6a). Increased absorption intensity and red shift suggests that at higher silver sputtering power we have larger silver nanoparticles with decreased nanoparticle to nanoparticle distance due to higher density of silver nanoparticles in agreement with TEM observations. However, when matrix thickness of the coating was increased while keeping silver sputtering power constant at 50 W, the silver nanoparticles again showed bimodal size distribution due to decrease in silver nanoparticles size. The increase in matrix thickness from 150 nm to 300 and 400 nm for silver sputtering power of 50 W (300 nm-50 W and 400 nm-50 W) brought the overall silver filling factor approximately to the same level as that obtained for 30 W (for 300 nm-50 W) and 15 W (for 400 nm-50 W) although the total silver concentration within the thin films was higher at higher power (at 50 W). Therefore, the absorption peaks both at 345 nm and 420 nm appeared again (300 nm-50 W and 400 nm-50 W in Fig. 6b). However, the transmittance level of the coatings with similar silver filling factors but different total silver amount in the nanocomposite (for example 150 nm-15 W and 400 nm-50 W) was different. The coating with higher silver concentration can absorb more than that with lower silver concentration (Brunon et al. 2011). This implies that the transparency of the nanocomposite film can be increased to certain extent by increasing the matrix

amount; **b** varied thickness of the films (150 nm, 300 nm and 400 nm) with constant deposition rate of silver

thickness while maintaining higher silver concentration within the thin film. However, it cannot be brought to the level of the thin film having lower silver concentration although both thin films may have same silver filling factor with respect to total volume of the thin film. The images of cotton fabric coated with nanocomposite thin films are shown in Fig. 7 which demonstrate variation in the color of the fabric under different deposition conditions. Maximum preservation of the original look of the fabric can be seen for fabric sample CF-150 nm-15 W which is deposited with minimum silver concentration. Whereas maximum color variation occurred for fabric sample CF-150 nm-50 W that contains maximum silver concentration deposited at 50 W. However, this variation in color with maximum silver concentration was restored to reasonable extent for samples CF-300 nm-50 W and CF-400 nm-50 W which contain same silver concentration dispersed in a thicker matrix.

Silver concentration and silver ions release

The total amount of silver deposited onto cotton fabric under three silver sputtering powers, namely 15 W, 30 W and 50 W (CF-150 nm-15 W, CF-150 nm-30 W and CF-150 nm-50 W), was determined via ICP-MS to be 55, 129 and 286 ppm (mg of silver per kg of fabric) respectively. For other two samples (CF-300 nm-50 W and CF-400 nm-50 W), the silver sputtering power was maintained at 50 W similar to

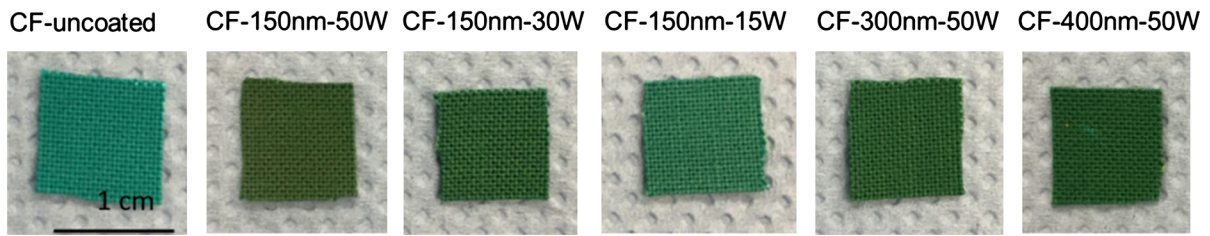


Fig. 7 Photographs of fabric samples coated with nanocomposite thin films prepared under various deposition conditions

CF-150 nm-50 W, therefore, these samples are also expected to contain same amount of silver (286 ppm) as that of sample CF-150 nm-50 W. However, in samples CF-300 nm-50 W and CF-400 nm-50 W, this silver amount is dispersed in a thicker matrix. It is of interest to evaluate the potential of these nanocomposite coatings to release silver ions in wet environment.

In aqueous environments, silver nanoparticles are oxidized and release silver cations (Ag^+). Antibacterial activity of silver nanoparticles is considered to be associated with release of silver ions from the coating (Körner et al. 2010). Thus, a controlled and sustained release of silver ions from the coating may contribute to sustained and prolonged antibacterial activity. Therefore, silver ion release behaviour of the deposited antibacterial coatings was evaluated by immersing the coated fabric samples in water and results are shown in Fig. 8. The Figure shows silver ion release profiles from the coated fabric dependent on immersion time, silver concentration as well as coating

thickness. It is worth mentioning that no abrupt release was observed in any case after immersing the sample in water. This is the benefit of embedding silver nanoparticles in the matrix which controls the release of silver ions into the aqueous environment. Direct exposure of the silver nanoparticles to the water may cause an abrupt release of silver ions in water (Kuzminova et al. 2016).

The graph shows that higher the silver concentration in a given coating thickness (Fig. 8a) (obtained at higher silver sputtering power), higher is the release of silver ions. On the other hand, increasing the coating thickness while keeping the silver concentration per unit fabric area the same (Fig. 8b, samples CF-150 nm-50 W, CF-300 nm-50 W and CF-400 nm-50 W) results in decrease in the release of silver ions. This implies that increased thickness of the matrix reduced the kinetics of silver ions release. It should be noted that all the samples in Fig. 8b were deposited at same silver sputtering power (50 W) thus containing approximately same concentration of silver on unit

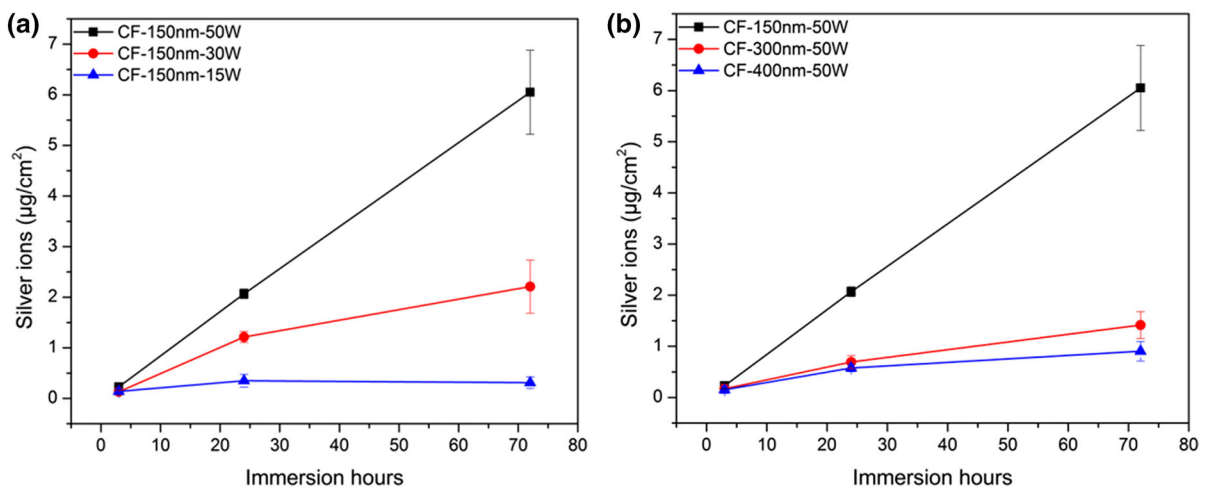


Fig. 8 Silver ion release profiles for cotton fabric coated with nanocomposite thin films. The measurements were carried via ICP-MS on water samples drawn after 3, 24 and 72 h of immersion in water

fabric surface area but dispersed in the coating matrix of varying thickness. This concentration was measured to be 286 ppm i.e. mg of silver per kg of cotton fabric via ICP-MS.

The cumulative release of Ag^+ both from CF-150 nm-50 W and CF-150 nm-30 W was more than 90% of the total deposited silver within 3 days of immersion in water. Whereas, it was 30, 23 and 15% from CF-150 nm-15 W, CF-300 nm-50 W and CF-400 nm-50 W respectively. The release of silver ions from (CF-150 nm-30 W) is higher than that from CF-300 nm-50 W and CF-400 nm-50 W despite the fact that concentration of silver deposited at 30 W is less than that deposited at 50 W. This indicates that higher thickness of the coating (matrix) suppressed the release of silver ions even if the concentration of silver per unit fabric area was higher than that in relatively thinner coating. This justifies the hypothesis that dispersing relatively higher silver concentration in thicker coating will provide more sustained supply of silver ions extending the life of the coated fabric in repeated use along with benefit of reduced coloration (due to smaller particle size) as mentioned earlier. This is of particular importance keeping in view that the controlled release of metal ions is considered very difficult to achieve as it is not only dependent on the concentration of metal particles. Hydrophobic nature of the matrix (discussed later in the article) is also responsible in suppressing the release of silver ions from the thicker matrices as has also been reported by Kylián et al. (2017). Other factors like surface roughness, surface oxidation kinetics and particle agglomeration state are also key factors to control the release rate of metal ions (Ponomarev et al. 2018).

Antibacterial performance

Silver nano particles are well known antimicrobial agents which demonstrate biocidal action against a wide variety of bacteria, both Gram positive and Gram negative, as well as fungi (Balagna et al. 2012) along with low cytotoxicity and absence of drug resistance (Wu et al. 2018). The exact mechanism for biocidal action of silver nano particles, as well as other metal nano particles, is not yet completely understood. However, experimental evidence suggests that antimicrobial activity of silver nano particles is associated with silver ions and hence on the kinetic of silver ions release from the silver nano particles (Ponomarev

et al. 2018). In this study, antibacterial activity of the prepared coatings was evaluated against *Staphylococcus epidermidis* and results are shown in Fig. 9. The Figure shows that, compared with the untreated control sample (CF-uncoated), where bacterial growth is well visible under fabric surface, all the coated samples showed antibacterial activity against *S. epidermidis*. However, the size of the inhibition halo is different for different samples.

In case of higher silver ion release from the coating (CF-150 nm-50 W and CF-150 nm-30 W), a well-defined inhibition halo can be seen around the samples. This indicates higher concentration of the active agent leached from the sample into the surrounding medium. As shown in Fig. 8, the minimum concentration of silver ions was released from CF-150 nm-15 W which also contains minimum silver concentration as compared with other samples. It can be observed that there wasn't bacterial growth under the fabric sample despite the absence of a well-defined inhibition halo. For the samples CF-300 nm-50 W and CF-400-50 W, which contain the same concentration of silver as that of CF-150 nm-50 W, but dispersed in thicker matrices, a very small inhibition halo can be observed. This is due to a more controlled release of silver ions from the thicker coating, CF-300 nm-50 W and CF-400-50 W, than from the thinner CF-150 nm-50 W. The formation of the inhibition halo depends on the leaching of the antimicrobial agent in the surrounding medium (Tomšič et al. 2008). This fact decreases the antibacterial agent concentration on the fabric surface and, consequently, diminishes the subsequent antimicrobial performances. Therefore, controlled release of silver ions will be more sustainable to maintain antibacterial activity for longer times. In addition, compared with other metal ions, silver gives bactericidal action at very low concentrations (Ponomarev et al. 2018). This property of silver nanoparticles combined further with controlled release can be useful for many other applications where cytotoxicity can be a concern while obtaining antibacterial activity for example in wound dressings or where the silver nanoparticle containing coating is in direct contact with human skin.

In order to assess the washing stability of the coating, antibacterial performance was also evaluated on samples subjected to multiple washing cycles. For this purpose, fabric samples CF-150 nm-50 W were

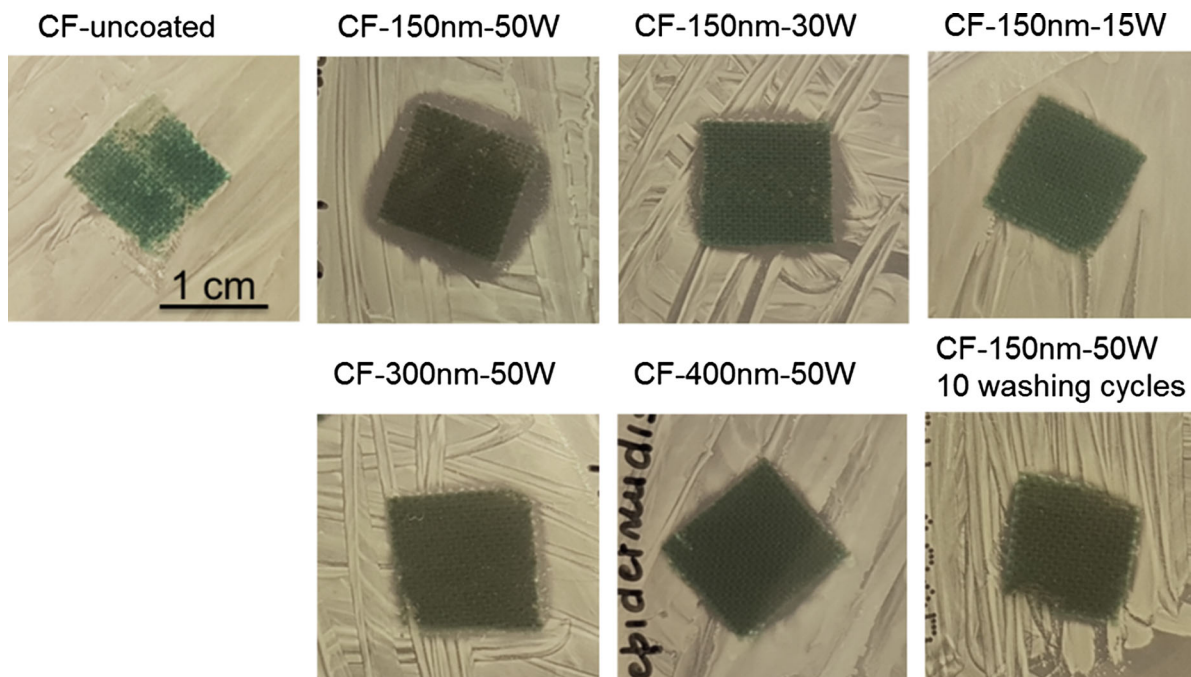


Fig. 9 Inhibition halo test on cotton samples deposited with nanocomposite thin films with varying silver concentration and coating thickness. Antibacterial activity was present even after 10 washing cycles

washed 10 times and subjected to the “Inhibition halo test”. Figure 9 shows that, although the size of the inhibition halo decreased after the washing treatment, the antibacterial activity was still present, in fact no microbial growth, under the sample surface, was observed. The washing stability of the thin films sputtered on textile surfaces has been found to be poor as reported by Wang et al. (2010). The results of this study show that reasonable washing stability for textiles deposited with sputtered thin films can be obtained.

Water wettability

Cotton fibers are hydrophilic due to abundance of hydroxyl groups in its structure that make cotton fabrics stain easily when in contact with liquids. Polysiloxanes are low surface energy polymers and thus make the surfaces hydrophobic on which they are applied. Fabric surfaces treated with polysiloxanes may result in high hydrophobicity to super hydrophobicity (Hao et al. 2016). Hydrophobicity of the cotton fabric coated by silver nanoparticles-plasma polymer thin film was assessed through water contact angle test and results are shown in Fig. 10. Uncoated cotton

fabric showed a water contact angle of 125° . High water contact angle on uncoated cotton fabric was due to dense weave structure of the fabric which may lead to higher water contact angle due to surface patterning and roughness. After deposition, the water contact angle increased from 125° up to 146° making the fabric surface highly hydrophobic, closer to super hydrophobicity.

Conclusion

In summary, an antibacterial, highly hydrophobic and semi transparent nanocomposite thin film was deposited on green colored cotton fabric intended to be used in medical wear. The nanocomposite thin film, composed of silver nano particles embedded in the plasma polymer matrix, was obtained via ecofriendly plasma based co-deposition scheme. Polymer matrix was obtained by polymerizing HMDSO monomer and its subsequent deposition on the substrate. The coating was deposited under five different deposition conditions mainly to vary the silver concentration and its size distribution within the polymer matrix to influence optical properties as well controlling the leaching

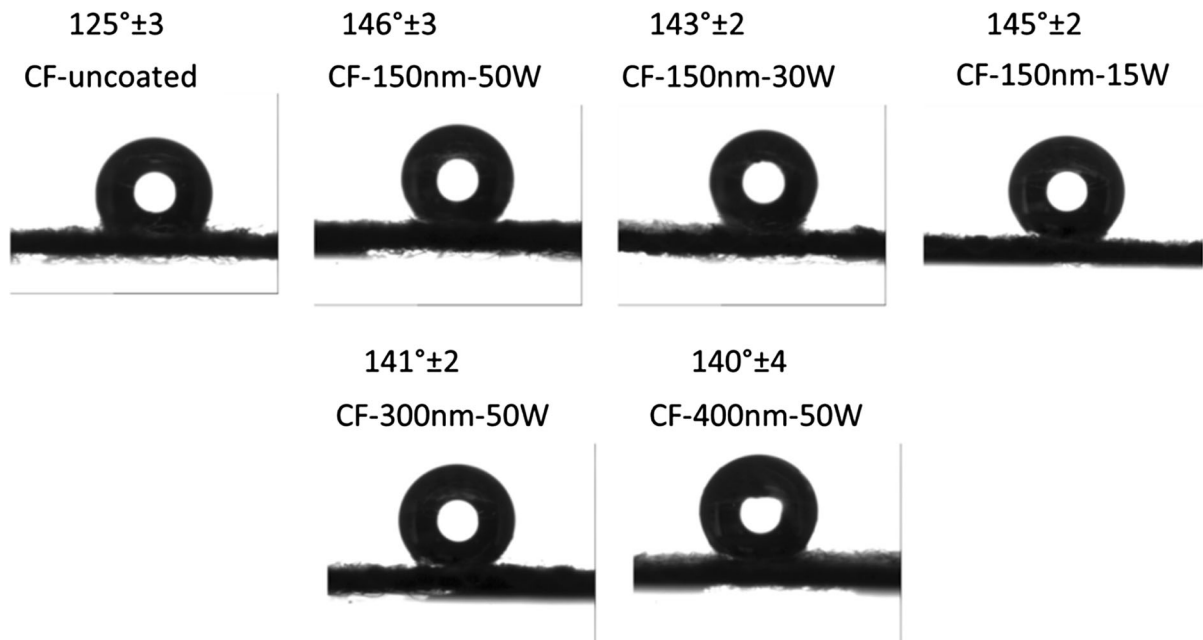


Fig. 10 Water contact angle on cotton fabric coated with nanocomposite thin films showing highly hydrophobic surface after coating

of silver ions. Silver concentration was varied either by decreasing silver deposition power without changing plasma polymer matrix thickness or by increasing plasma polymer matrix thickness without changing silver deposition power. Thickness of the plasma polymer was found to be more important in controlling the release of ionic silver in aqueous medium along with reduction in optical absorbance. While decreasing silver deposition power without changing polymer matrix resulted in more transparent coating due to lower silver concentration and smaller sized particles. Thus variation in the silver concentration or matrix thickness led to the variation in the silver nano particle size and their distribution within the coating matrix which consequently influenced the optical properties as well as silver ions release from the coating. The deposition resulted in bimodal distribution of silver nano particles where silver concentration was lower or matrix thickness was higher. The thin films deposited under all the five conditions demonstrated effective antibacterial activity against *S. epidermidis* LMG 10474 in the “Inhibition halo test”. with size of the halo depending upon silver ion release profiles from the respective coatings. The coating showed a certain degree of washing stability as it was able to retain antibacterial activity when subjected to 10 washing cycles. The coating rendered the surface of the cotton

fabric high hydrophobicity reaching water contact angle as high as 146°. This work shows that independent manipulation of the process parameters for silver and plasma polymer in the co-deposition scheme can yield nano composite coatings comprising silver nano particles with acceptable transparency and long term antibacterial properties for practical applications.

References

- Alexander MR, Short RD, Jones FR, Stollenwerk M, Zabold J, Michaeli W (1996) An X-ray photoelectron spectroscopic investigation into the chemical structure of deposits formed from hexamethyldisiloxane/oxygen plasmas. *J Mater Sci* 31:1879–1885
- Ali SW, Purwar R, Joshi M, Rajendran S (2014) Antibacterial properties of Aloe vera gel-finished cotton fabric. *Cellulose* 21:2063–2072
- Bakr O, Amendola V, Aikens C, Wenseleers W, Li R, Negro LD, Schatz GC, Stellacci F (2009) Silver nanoparticles with broad multiband linear optical absorption. *Angew Chem* 121:6035–6040
- Balagna C, Perero S, Ferraris S, Miola M, Fucale G, Manfredotti C, Battiato A, Santella D, Vernè E, Vittone E, Ferraris M (2012) Antibacterial coating on polymer for space application. *Mater Chem Phys* 135:714–722
- Beyene H, Tichelaar F, Peeters P, Kolev I, Sanden M, Creatore M (2010) Hybrid sputtering-remote PECVD deposition of Au nanoparticles on SiO₂ layers for surface plasmon

- resonance-based colored coatings. *Plasma Process Polym* 7:657–664
- Brunon C, Chadeau E, Oulahal N, Grossiord C, Dubost L, Bessueille F (2011) Characterization of plasma enhanced chemical vapor deposition-physical vapor deposition transparent deposits on textiles to trigger various antimicrobial properties to food industry textiles. *Thin Solid Films* 519:5838–5845
- Chadeau E, Oulahal N, Dubost L, Favergeon F, Degraeve P (2010) Anti-listeria innocua activity of silver functionalised textile prepared with plasma technology. *Food Control* 21:505–512
- Deng X, Leys C, Vujosevic D, Vuksanovic V, Uros Cvelbar DG, Morent R et al (2014) Engineering of composite organosilicon thin films with embedded silver nanoparticles via atmospheric pressure plasma process for antibacterial activity. *Plasma Process Polym* 11:921–930
- Despax B, Raynaud P (2007) Deposition of “polysiloxane” thin films containing silver particles by an RF asymmetrical discharge. *Plasma Process Polym* 4:127–134
- Drábik M, Pešička J, Biederman H, Hegemann D (2015) Long-term aging of Ag/a-C:H:O nanocomposite coatings in air and in aqueous environment. *Sci Technol Adv Mater* 16:2
- El-Nahhal I, Elmanama A, Amara N, Qodih F, Selmane M, Chehimi M (2018) The efficacy of surfactants in stabilizing coating of nano-structured CuO particles onto the surface of cotton fibers and their antimicrobial activity. *Mater Chem Phys* 215:221–228
- Fei Z, Liu B, Zhu M, Wang W, Yu D (2018) Antibacterial finishing of cotton fabrics based on thiol-maleimide click chemistry. *Cellulose* 25:3179–3188
- Foksoiewicz-Flaczyk J, Walentowska J, Przybylak M, Maciejewski H (2016) Multifunctional durable properties of textile materials modified by biocidal agents in the sol-gel process. *Surf Coat Technol* 304:160–166
- Gao Y, Cranston R (2010) An effective antimicrobial treatment for wool using polyhexamethylene biguanide as the biocide, part 1: biocide uptake and antimicrobial activity. *J Appl Polym Sci* 117:3075–3082
- Gharibshahi L, Saion E, Gharibshahi W, Shaari AM (2017) Structural and optical properties of Ag nanoparticles synthesized by thermal treatment method. *Materials* 10:402
- Ghayempour S, Montazer M (2017) Ultrasound irradiation based in situ synthesis of star-like Tragacanth gum/zinc oxide nanoparticles on cotton fabric. *Ultrason Sonochemistry* 34:458–465
- Hanus J, Drábik M, Hlíděk P, Biederman H, Radnoczi G, Slavínska D (2009) Some remarks on Ag/C: H nanocomposite films. *Vacuum* 83:454–456
- Hao L, Gao T, Xu W, Wang X, Yang S, Liu X (2016) Preparation of crosslinked polysiloxane/SiO₂ nanocomposite via in-situ condensation and its surface modification on cotton fabrics. *Appl Surf Sci* 371:281–288
- Hlíděk P, Biederman H, Choukourov A, Slavínská D (2009) Behavior of polymeric matrices containing silver inclusions, 2-oxidative aging of nanocomposite Ag/C: H and Ag/C: H: O films. *Plasma Process Polym* 6:34–44
- ImageJ: <https://imagej.nih.gov/ij/>
- Irfan M, Perero S, Miola M, Maina G, Ferri A, Ferraris M et al (2017) Antimicrobial functionalization of cotton fabric with silver nanoclusters/silica composite coating via RF co-sputtering technique. *Cellulose* 24:2331–2345
- Jamuna-Thevi K, Bakar SA, Ibrahim S, Shahab N, Toff MRM (2011) Quantification of silver ion release, in vitro cytotoxicity and antibacterial properties of nanostructured Ag doped TiO₂ coatings on stainless steel deposited by RF magnetron sputtering. *Vacuum* 86:235–241
- Körner E, Aguirre M, Fortunato G, Ritter A et al (2010) Formation and distribution of silver nanoparticles in a functional plasma polymer matrix and related Ag⁺ release properties. *Plasma Process Polym* 7:619–625
- Kratochvíl J, Štěřba J, Lieskovská J, Langhansová H, Kuzminova A, Khalakhan I, Kylián O, Straňák V (2018) Antibacterial effect of Cu/C: F nanocomposites deposited on PEEK substrates. *Mater Lett* 230:96–99
- Kuzminova A, Beranová J, Polonskyi O, Shelemin A, Kyliána O, Choukourov A (2016) Antibacterial nanocomposite coatings produced by means of gas aggregation source of silver nanoparticles. *Surf Coat Technol* 25:225–230
- Kylián O, Kratochvíl J, Petr M, Kuzminova A, Slavínská Danka, Biederman H (2017) Ag/C: F Antibacterial and hydrophobic nanocomposite coatings. *Funct Mater Lett* 10:1–4
- Lin J, Chen X, Chen C, Hu J, Zhou C, Cai X et al (2018) Durably antibacterial and bacterially antiadhesive cotton fabrics coated by cationic fluorinated polymers. *Appl Mater Interfaces* 10:6124–6136
- Liu Y, Li J, Cheng X, Ren X, Huang T (2015) Self-assembled antibacterial coating by N-halamine polyelectrolytes on a cellulose substrate. *J Mater Chem B* 3:1446–1454
- Mariselvam R, Ranjitsingh R, Selvakumar M, Krishnamoorthy R, Alshatwi A (2017) Eco friendly natural dyes from *Syzygium cumini* (L) (Jambolan) Fruit seed endosperm and to preparation of antimicrobial fabric and their washing properties. *Fibers Polym* 18:460–464
- Moulder J, Chastain J (1992) Handbook of x-ray photoelectron spectroscopy: a reference book of standard spectra for identification and interpretation of XPS data. Physical Electronics Division, Perkin-Elmer Corporation, Waltham
- Perelshstein I, Lipovsky A, Perkas N, Tzanov T, Arguirova M, Leseva M (2015) Making the hospital a safer place by sonochemical coating of all its textiles with antibacterial nanoparticles. *Ultrason Sonochemistry* 25:82–88
- Peter T, Wegner M, Zaporojtchenko V, Strunskus T, Bornholdt S, Kersten H et al (2011) Metal/polymer nanocomposite thin films prepared by plasma polymerization and high pressure magnetron sputtering. *Surf Coat Technol* 205:S38–S41
- Pitsitsak P, Ruktanonchai U (2014) Preparation, characterization, and in vitro evaluation of antibacterial sol–gel coated cotton textiles with prolonged release of curcumin. *Text Res J* 85:949–959
- Ponomarev V, Sukhorukova I, Sheveyko A, Permyakova E, Manakhov A, Ignatov S et al (2018) Antibacterial performance of TiCaPCON Films incorporated with Ag, Pt, and Zn: bactericidal ions versus surface microgalvanic interactions. *Appl Mater Interfaces* 10:24406–24420
- Radeva E, Georgieva V, Lazarov J, Gadjanova V, Tsankov D (2014) Plasma polymerized hexamethyldisiloxane thin films for NO₂ gas sensor application. *Dig J Nanomater Biostructures* 9:459–466

- Ramirez D, Jaramillo F (2018) Improved mechanical and antibacterial properties of thermoplastic polyurethanes by efficient double functionalization of silver nanoparticles. *J Appl Polym Sci* 135:46180
- Rau C, Kulisch W (1994) Mechanisms of plasma polymerization of various silico-organic monomers. *Thin Solid Films* 249:28–37
- Saulou C, Despax B, Raynaud P, Zanna S, Seyeux A, Marcus P et al (2012) Plasma-mediated nanosilver-organosilicon composite films deposited on stainless steel: synthesis, surface characterization, and evaluation of anti-adhesive and anti-microbial properties on the model yeast *Saccharomyces cerevisiae*. *Plasma Process Polym* 9:324–338
- Savoia D (2012) Plant-derived antimicrobial compounds: alternatives to antibiotics. *Future Microbiol* 7:979–990
- Schmittgens R, Wolf M, Schultheiss E (2009) A versatile system for large area coating of nanocomposite thin films. *Plasma Process Polym* 6:S912–S916
- Stawski D, Sahariah P, Hjálmarsson M, Wojciechowska D, Puchalski M, Másson M (2016) N, N, N-trimethyl chitosan as an efficient antibacterial agent for polypropylene and polylactide nonwovens. *J Text Inst* 108:1041–1049
- Tomšič B, Simončič B, Orel B, Černe L, Tavčer P, Zorko M et al (2008) Sol–gel coating of cellulose fibres with antimicrobial and repellent properties. *J Sol Gel Sci Technol* 47:44–57
- Wang RX, Tao XM, Wang Y, Wang GF, Shang SM (2010) Microstructures and electrical conductance of silver nanocrystalline thin films on flexible polymer substrates. *Surf Coat Technol* 204:1206–1210
- Wiley BJ, Im SH, Li Z-Y, McLellan J, Siekkinen A, Xia Y (2006) Maneuvering the surface plasmon resonance of silver nanostructures through shape-controlled synthesis. *J Phys Chem* 110:15666–15675
- Wu T, Lu F, Wen QY, Lu B, Rong B, Dai F et al (2018) Ovel strategy for obtaining uniformly dispersed silver nanoparticles on soluble cotton wound dressing through carboxymethylation and in situ reduction: antimicrobial activity and histological assessment in animal model. *Cellulose* 25:5361–5376
- Xu Q, Xie L, Diao H, Li F, Zhang Y, Fu F et al (2017) Antibacterial cotton fabric with enhanced durability prepared using silver nanoparticles and carboxymethyl chitosan. *Carbohydr Polym* 177:187–193
- Zemljic L, Peršin Z, Šauperl O, Rudolf A, Kostić M (2017) Medical textiles based on viscose rayon fabrics coated with chitosan-encapsulated iodine: antibacterial and antioxidant properties. *Text Res J* 88:2519–2531

Publisher's Note Springer Nature remains neutral with regard to jurisdictional claims in published maps and institutional affiliations.